

Blue-tilted inflationary tensor spectrum and reheating in the light of NANOGrav results

Sachiko Kuroyanagi^{1,2}, Tomo Takahashi³ and Shuichiro Yokoyama^{4,5}

¹*Instituto de Física Teórica UAM-CSIC, Universidad Autónoma de Madrid,
Cantoblanco, 28049 Madrid, Spain*

²*Department of Physics, Nagoya University, Nagoya, Aichi 464-8602, Japan*

³*Department of Physics, Saga University, Saga 840-8502, Japan*

⁴*Kobayashi Maskawa Institute, Nagoya University, Aichi 464-8602, Japan*

⁵*Kavli Institute for the Physics and Mathematics of the Universe (WPI),
Todai institute for Advanced Study, University of Tokyo, Kashiwa, Chiba 277-8568,
Japan*

Abstract

We discuss the possibility of explaining the recent NANOGrav results by inflationary gravitational waves (IGWs) with a blue-tilted primordial spectrum. Although such IGWs can account for the NANOGrav signal without contradicting the upper bound on the tensor-to-scalar ratio at the cosmic microwave background scale, the predicted spectrum is in strong tension with the upper bound on the amplitude of the stochastic gravitational wave background by big-bang nucleosynthesis (BBN) and the second LIGO-Virgo observation run. However, the thermal history of the Universe, such as reheating and late-time entropy production, affects the spectral shape of IGWs at high frequencies and permits evading the upper bounds. We show that, for the standard reheating scenario, when the reheating temperature is relatively low, a blue tensor spectrum can explain the recent NANOGrav signal without contradicting the BBN and the LIGO-Virgo constraints. We further find that, when one considers a late-time entropy production, the NANOGrav signal can be explained even for an instant reheating scenario.

1 Introduction

Stochastic gravitational wave background (SGWB) can be used as a powerful probe of the Universe. Many possible sources of SGWB, both from cosmological and astrophysical processes, have been suggested and investigated rigorously (see, e.g., [1] and references therein). If a SGWB was detected, it would provide important implications for cosmology and astrophysics.

Recently, the North American Nanohertz Observatory for Gravitational Waves (NANOGrav) has reported a possible detection of a SGWB with their 12.5 year data set of the pulsar timing array [2]. Although one needs a confirmation of quadrupolar spatial correlations to claim the detection of a SGWB [3], the NANOGrav results have already stimulated a lot of work to pursue a possible source of the cosmological signal [4–25].

Among various sources of SGWB, the inflationary gravitational waves (IGWs) are one of the most interesting sources to explore as a possible explanation of the recent NANOGrav results. In the inflationary Universe, not only the scalar fluctuations, which source the cosmic large-scale structure, but also the tensor fluctuations, which could be observed as a SGWB, are generated from quantum fluctuations of spacetime. The IGWs naturally have a broad power spectrum, whose amplitude depends on the inflationary model. Since the IGWs on large scales (corresponding the frequency of $\sim 10^{-16}\text{Hz}$) can be well constrained by cosmic microwave background (CMB), one needs a blue-tilted tensor spectrum to explain the NANOGrav results at $\sim 10^{-8}\text{Hz}$ without contradicting the upper bound on the tensor-to-scalar ratio obtained by recent CMB experiments, such as the Planck satellite. Although it is generally difficult to realize such a blue-tilted tensor spectrum in the standard slow-roll inflation in general relativity, possible models have been proposed and discussed in the context of modified theories of gravity or non-standard inflation models (see, e.g., [25–36]).

When considering a blue-tilted tensor spectrum, we also need to check whether the spectral amplitude at high frequencies (above $\sim 10^{-10}\text{Hz}$) is consistent with the big-bang nucleosynthesis (BBN) bound on an extra radiation component. Furthermore, the LIGO-Virgo interferometer network currently provides a tighter upper bound on the SGWB amplitude at the frequency of $\sim 100\text{ Hz}$.^{#1} In fact, the constraints on the SGWB with a blue-tilted spectrum by BBN and LIGO-Virgo are quite strong and hence it is nontrivial to determine whether IGWs can explain the recent NANOGrav signal without conflicting with the BBN and LIGO-Virgo constraints, which is the issue we will investigate in this paper.

As the simplest thermal history of the Universe, one can consider the case where reheating occurred instantaneously just after inflation. In this case, a blue-tilted spectrum for explaining the NANOGrav result is ruled out by the BBN constraint, as has been

^{#1}Scalar fluctuations can be induced by IGWs through non-linear (second-order) effects, which can lead to the overproduction of primordial black holes (PBHs). Thus, the current upper bounds on the abundance of PBHs can also provide comparable constraints on the amplitude of the IGWs at relatively higher frequency region [37, 38].

pointed out in [14, 21]. However, in the conventional scenario of reheating, the oscillating inflaton-dominated phase, where the expansion of the background Universe behaves like that in a matter-dominated (MD) era, lasts for a certain period of time after inflation, followed by the radiation-dominated (RD) Universe. It has been shown that the power spectrum of the IGWs which re-entered the horizon during a MD phase get suppressed by a frequency dependence of $\propto f^{-2}$ [39–45], while the modes which entered the horizon during the RD phase have a dependence $\propto f^0$. Thus, by considering an early MD phase after inflation, the GW amplitude at high frequencies can be reduced, which enables us to evade the BBN and LIGO-Virgo constraints. Therefore, the model of reheating significantly affects constraints on the tensor spectral index n_t by BBN and LIGO-Virgo [46]. Indeed, as we will see in this paper, for example if we assume the tensor-to-scalar ratio $r = 0.06$ at the CMB scale, a blue-tilted spectrum can explain the NANOGrav signal without contradicting the upper bounds from BBN and LIGO-Virgo, when the reheating temperature is lower than $T \simeq 10^3$ GeV.

Furthermore, in some scenarios of the early Universe, late-time entropy production can occur due to the existence of a scalar field such as a modulus. In this case, an early MD phase is realized after the RD period followed by reheating due to the inflaton. Namely, in this scenario, MD phases appear twice between the end of inflation and the BBN epoch, which accordingly makes the GW spectra different from the case of the standard thermal history [47–49]. As mentioned above, the GW spectrum gets suppressed for the modes which entered the horizon during MD phase, and thus the constraints from BBN and LIGO-Virgo can be alleviated by late-time entropy production as well [46]. We will see that, if the duration of the late-time entropy production is long enough, even IGWs with instant reheating at $T_R \sim 10^{15}$ GeV can explain the NANOGrav signal while satisfying the constraints from BBN and LIGO-Virgo.

The structure of this paper is the following. In the next section, we briefly summarize the formulas to calculate the spectrum of IGWs and how IGWs with a blue-tilted spectrum are constrained by the BBN and the LIGO-Virgo upper bounds. In Section 3, we discuss the possibility of explaining the NANOGrav result with IGWs with a blue-tilted spectrum by taking into account reheating and late-time entropy production, and then explore the parameter space allowed by both BBN and LIGO-Virgo. The last section is devoted to conclusion.

2 The spectrum of IGWs and upper bounds by BBN and LIGO-Virgo

Here we briefly summarize the formulas to calculate the spectrum of IGWs and upper bounds on the amplitude of the SGWB by BBN and the LIGO-Virgo interferometer network. For details, see Ref. [46] and the references therein.

2.1 The spectrum of IGWs

GWs are described as tensor metric perturbations $h_{ij}(\tau, \mathbf{x})$ in the flat Friedmann-Lemaître-Robertson-Walker background:

$$ds^2 = a(\tau) \left[-d\tau^2 + (\delta_{ij} + h_{ij}(\tau, \mathbf{x})) dx^i dx^j \right], \quad (2.1)$$

where τ is the conformal time, $a(\tau)$ is the scale factor, and h_{ij} satisfies the transverse-traceless condition, $\partial^i h_{ij} = h^i_i = 0$. Using the Fourier transformation,

$$h_{ij}(\tau, \mathbf{x}) = \sum_{\lambda} \int \frac{dk^3}{(2\pi)^{3/2}} e^{i\mathbf{x}\cdot\mathbf{k}} \epsilon_{ij}^{\lambda}(\mathbf{k}) h_{\mathbf{k}}^{\lambda}(\tau), \quad (2.2)$$

with $\epsilon_{ij}^{\lambda}(\mathbf{k})$ being the polarization tensor, the energy density of GWs can be written as

$$\rho_{\text{GW}} = \frac{1}{32\pi G} \int d\ln k \left(\frac{k}{a} \right)^2 \frac{k^3}{\pi^2} \sum_{\lambda} |h_{\mathbf{k}}^{\lambda}|^2. \quad (2.3)$$

By defining the power spectrum of primordial tensor perturbations generated during inflation as

$$\mathcal{P}_{T,\text{prim}}(k) = \frac{k^3}{\pi^2} \sum_{\lambda} |h_{\mathbf{k},*}^{\lambda}|^2, \quad (2.4)$$

where $*$ denotes the value at the end of inflation,^{#2} one can write down the GW energy density parameter today as

$$\Omega_{\text{GW}} \equiv \frac{1}{\rho_{\text{crit}}} \frac{d\rho_{\text{GW}}}{d\ln k} = \frac{1}{12} \left(\frac{k}{a_0 H_0} \right)^2 T_T^2(k) \mathcal{P}_{T,\text{prim}}(k), \quad (2.5)$$

where $\rho_{\text{crit}} = 3H_0^2/(8\pi G)$ is the critical density of the universe and $T_T(k)$ is the transfer function, which is defined as $T_T^2(k) = |h_{\mathbf{k},0}^{\lambda}|^2/|h_{\mathbf{k},*}^{\lambda}|^2$ with 0 denoting the value at the present time.

The primordial tensor spectrum, $\mathcal{P}_{T,\text{prim}}(k)$, is often parameterized as

$$\mathcal{P}_{T,\text{prim}}(k) = A_T \left(\frac{k}{k_{\text{ref}}} \right)^{n_T}, \quad (2.6)$$

where A_T is the amplitude at a reference scale k_{ref} and n_T is the tensor spectral index. The amplitude of the primordial tensor perturbations at the CMB scale is commonly characterized by the tensor-to-scalar ratio r as

$$r \equiv \frac{\mathcal{P}_{T,\text{prim}}(k_{\text{ref}})}{\mathcal{P}_{\zeta}(k_{\text{ref}})}, \quad (2.7)$$

^{#2}Here, for simplicity, we assume that the tensor perturbations on super-horizon scales stay constant in time after the end of inflation. In case where the super-horizon tensor perturbations evolve even after the end of inflation, we need to modify the transfer function, $T_T(k)$, which will be given by Eqs. (2.8) and (2.15).

where $\mathcal{P}_\zeta(k)$ is the primordial power spectrum of scalar perturbations. Although n_T can also be a scale-dependent variable, we assume it to be constant in this paper.^{#3}

For the transfer function $T_T(k)$, we use the following fitting formulas. In the case of the standard reheating scenario, the universe experiences a MD (inflation ϕ oscillation-dominated) phase after inflation and the RD phase follows. In this case, the transfer function is given by [41, 46, 51]:

$$T_T^2(k) = \Omega_m^2 \left(\frac{g_*(T_{k,\text{in}})}{g_{*0}} \right) \left(\frac{g_{*0}}{g_{*s}(T_{k,\text{in}})} \right)^{4/3} \left(\frac{3j_1(k\tau_0)}{k\tau_0} \right)^2 T_1^2(x_{\text{eq}}) T_2^2(x_R) \quad (2.8)$$

(Standard reheating scenario),

where Ω_m is the present day energy density parameter for matter, $T_{k,\text{in}}$ denotes the temperature at the time when mode k enters the horizon, and $g_*(T)$ and $g_{*s}(T)$ are the relativistic degrees of freedom and its counterpart for entropy, respectively. The subscript 0 denotes the value at the present time, and we use $g_{*0} = 3.36$ and $g_{*s0} = 3.91$. In the limit of $k\tau_0 \rightarrow 0$, the spherical Bessel function can be approximated as $j_1(k\tau_0) \approx 1/\sqrt{2}k\tau_0$. The changes of $g_*(T)$ and $g_{*s}(T)$ affect the shape of the spectrum of IGWs [42, 52, 53] and we use the fitting formula proposed in Ref. [46],

$$g_*(T_{k,\text{in}}(k)) = g_{*0} \left(\frac{A + \tanh \left[-2.5 \log_{10} \left(\frac{k/(2\pi)}{2.5 \times 10^{-12} \text{ Hz}} \right) \right]}{A + 1} \right) \left(\frac{B + \tanh \left[-2.0 \log_{10} \left(\frac{k/(2\pi)}{6.0 \times 10^{-9} \text{ Hz}} \right) \right]}{B + 1} \right), \quad (2.9)$$

where

$$A = \frac{-1 - 10.75/g_{*0}}{-1 + 10.75/g_{*0}}, \quad B = \frac{-1 - g_{\text{max}}/10.75}{-1 + g_{\text{max}}/10.75}. \quad (2.10)$$

Here g_{max} is the maximum value for g_* and we take the sum of the standard model particles $g_{\text{max}} = 106.75$. The entropic counterpart $g_{*s}(T_{k,\text{in}})$ can be obtained by replacing g_{*0} with g_{*s0} in Eq. (2.9). The function $T_1(x)$ and $T_2(x)$ are the fitting formulas corresponding to the changes of the spectral shape due to the radiation-matter equality and reheating, and respectively given by

$$T_1^2(x) = 1 + 1.57x + 3.42x^2, \quad (2.11)$$

$$T_2^2(x) = (1 - 0.22x^{1.5} + 0.65x^2)^{-1}, \quad (2.12)$$

where $x_{\text{eq}} \equiv k/k_{\text{eq}}$ and $x_R \equiv k/k_R$ with

$$k_{\text{eq}} = 7.1 \times 10^{-2} \Omega_m h^2 \text{ Mpc}^{-1}, \quad (2.13)$$

$$k_R = 1.7 \times 10^{14} \left(\frac{g_{*s}(T_R)}{106.75} \right)^{1/6} \left(\frac{T_R}{10^7 \text{ GeV}} \right) \text{ Mpc}^{-1}. \quad (2.14)$$

^{#3}For higher-order correction to the scale dependence, see, e.g., [50].

Here each wavenumber corresponds to the mode which enters the horizon at the radiation-matter equality and the transition from the early MD phase to the RD phase, respectively, and T_R is the so-called reheating temperature, which is the temperature of the Universe when reheating completes and the RD phase starts.

In the scenario where the late-time entropy production occurs after reheating through the decay of an oscillating scalar field σ , the background evolution proceeds as MD (inflation ϕ oscillation-dominated) \rightarrow RD \rightarrow MD (σ -oscillation dominated) \rightarrow RD. In such a case, the transfer function is given by [46, 47]

$$T_T^2(k) = \Omega_m^2 \left(\frac{g_*(T_{k,\text{in}})}{g_{*0}} \right) \left(\frac{g_{*0}}{g_{*s}(T_{k,\text{in}})} \right)^{4/3} \left(\frac{3j_1(k\tau_0)}{k\tau_0} \right)^2 T_1^2(x_{\text{eq}}) T_2^2(x_\sigma) T_3^2(x_{\sigma R}) T_2^2(x_{R'}) \quad (2.15)$$

(Late-time entropy production scenario),

where $T_3^2(x)$ is the transfer function corresponding to the transition from the first RD phase to the σ -oscillation dominated phase and given by

$$T_3^2(x) = 1 + 0.59x + 0.65x^2. \quad (2.16)$$

Here we define $x_\sigma \equiv k/k_\sigma$ where k_σ corresponds to the mode entering the horizon at the time when σ decays into radiation, i.e., the second reheating, and is given by

$$k_\sigma = 1.7 \times 10^{14} \left(\frac{g_{*s}(T_\sigma)}{106.75} \right)^{1/6} \left(\frac{T_\sigma}{10^7 \text{ GeV}} \right) \text{ Mpc}^{-1}, \quad (2.17)$$

with T_σ being the temperature of the Universe when the decay of σ field completes. We also define $x_{\sigma R} = k/k_{\sigma R}$ and $x_{R'} = k/k_{R'}$, which are respectively given by

$$k_{\sigma R} = k_\sigma F^{2/3}, \quad k_{R'} = k_R F^{-1/3}, \quad (2.18)$$

where F characterizes the amount of entropy produced by the decay of σ and can be written as

$$F \equiv \frac{s(T_\sigma) a^3(T_\sigma)}{s(T_R) a^3(T_R)}, \quad (2.19)$$

with $s(T)$ being the entropy density. Here, $k_{\sigma R}$ corresponds to the mode entering the horizon when oscillating σ begins to dominate the Universe. For later discussion, we also define the temperature corresponding to $k_{\sigma R}$ as $T_{\sigma R}$. Note that the wavenumber corresponding to the end of first reheating is modified by the factor of $F^{-1/3}$ compared to the case without second reheating even for the same reheating temperature. We use the subscript R' instead of R in order to distinguish them.

By using the fitting formulas for the transfer functions given here, one can calculate the spectra of IGWs for scenarios with the standard reheating and late-time entropy production. Throughout the paper, we use the Planck 2018 cosmological parameters for a

flat Λ -CDM universe; $h = 0.6737$, $\Omega_m = 0.3147$, $\Omega_\Lambda = 1 - \Omega_m$, and $\ln(\mathcal{P}_\zeta 10^{10}) = 3.043$ at $k_{\text{ref}} = 0.05 \text{ Mpc}^{-1}$ [54]. The upper bound on the tensor-to-scalar ratio has been updated in the literature [55–57]. In the following, we use $r = 0.06$ at $k_{\text{ref}} = 0.05 \text{ Mpc}^{-1}$ as a reference upper bound for r on large scales [56].

2.2 BBN constraint

Primordial GWs contribute to the total energy density of extra relativistic species during BBN. In order not to spoil the BBN through the expansion rate of the Universe, ^{#4} the energy density of the SGWB should satisfy

$$\int_{f_1}^{f_2} d(\ln f) \Omega_{\text{GW}}(f) h^2 \leq 5.6 \times 10^{-6} \left(N_{\text{eff}}^{(\text{upper})} - 3 \right), \quad (2.20)$$

where $N_{\text{eff}}^{(\text{upper})}$ is the upper bound on the effective number of relativistic degrees of freedom. To evaluate the constraint from BBN, we adopt the 2σ upper limit for N_{eff} from BBN (observations of ^4He and D) as $N_{\text{eff}}^{(\text{upper})} = 3.41$ [58].

The lower limit of the integral in the left hand side is the frequency of the mode entering the horizon at the BBN epoch and we take $f_1 = 10^{-10} \text{ Hz}$. The upper limit of the integral f_2 corresponds to the highest frequency of GWs, which is determined by the Hubble expansion rate at the end of inflation, and given by

$$f_2 = \frac{a_{\text{end}} H_{\text{end}}}{2\pi} \approx 1.1 \times 10^8 \left(\frac{T_R}{10^{15} \text{ GeV}} \right)^{1/3} \left(\frac{H_{\text{end}}}{10^{14} \text{ GeV}} \right)^{1/3} F^{-1/3} \text{ Hz}. \quad (2.21)$$

Typically, when we consider the MD phase during reheating, the high-frequency IGWs are suppressed and do not contribute to the integral. Thus, although the value of f_2 has small dependencies on T_R , H_{end} and F , they do not affect the BBN constraint unless we consider instant reheating.

2.3 LIGO-Virgo constraint

Non-detection of a SGWB by the Advanced LIGO-Virgo detector network in the first and second observing run (O1 and O2) has provided an upper bound on the amplitude of the SGWB as [59]

$$\Omega_{\text{GW}} \leq 6.0 \times 10^{-8}, \quad (2.22)$$

at the reference frequency of $f_{\text{LV}} = 25 \text{ Hz}$ for a frequency-independent (flat) background. The frequency band containing 99% of the sensitivity is $f = 20 - 81.9 \text{ Hz}$ for O2.

^{#4}Although CMB can also put a constraint on an extra radiation component, in most analysis of CMB, the extra radiation component is implemented as a fluid similar to neutrino. However, fluctuations of the extra radiation originated from GWs behave differently from those of such a fluid and the evolution of fluctuations would be different, and hence we do not consider the constraint from CMB in this paper.

Note that this is an upper limit obtained for $\alpha = 0$, where α is a parameter to characterize the spectral tilt at the LIGO frequency, $\Omega_{\text{GW}} = \Omega_{\text{GW},\alpha}(f/f_{\text{LV}})^\alpha$. The upper limit changes for different values of α . In order to take this into account, we use the following formula adding the theoretically obtained α dependence (for details, see [46]),

$$\Omega_{\text{GW}} \leq 6.0 \times 10^{-8} \sqrt{\frac{5-2\alpha}{5}} \left(\frac{f_{\text{min}}}{f_{\text{LV}}}\right)^{-\alpha}, \quad (2.23)$$

where we take $f_{\text{min}} = 20\text{Hz}$.

3 Implications of the NANOGrav results for IGWs

Now we discuss implications of the recent NANOGrav results for IGWs with a blue-tilted spectrum. We calculate the spectra of IGWs and constraints from BBN and LIGO-Virgo by using the procedure presented in the previous section for the cases with the standard reheating and late-time entropy production scenario. Model parameters for the standard reheating scenario are: the amplitude of the IGWs, which we characterize by the tensor-to-scalar ratio r , the spectral index n_T , and the reheating temperature T_R . For the case of late-time entropy production scenario, in addition to r , n_T , and T_R , we also need to specify the second reheating temperature T_σ and the amount of entropy produced by the decay of the σ field, which is characterized by F .

In Fig. 1, the spectra of IGWs for some parameter sets are shown. In the left panel, we show the spectra for the standard reheating scenario, assuming $r = 0.06$ and $n_T = 0.85$, for different reheating temperatures $T_R = 10^{-1}, 1, 10$ GeV. In the right panel, we show the case of late-time entropy production, assuming $r = 0.06$, $n_T = 0.85$, $T_\sigma = 1$ GeV and $F = 10, 10^3, 10^6$ with $T_R = 10^5, 10^9, 10^{14}$ GeV, respectively. We also show the amplitude of the SGWB indicated by the recent NANOGrav result (orange colored region), and upper bounds by BBN (black dashed line) and LIGO-Virgo (black triangle).

In the following, we discuss whether IGWs with a blue-tilted spectrum can account for the recent NANOGrav signal without conflicting the constraints from BBN and LIGO-Virgo and investigate the parameter spaces.

3.1 Case with standard reheating

We start with the case of the standard reheating scenario. The NANOGrav results have been reported in terms of $h_c(f)$, the power spectrum of the characteristic GW strain which can be related to Ω_{GW} as $\Omega_{\text{GW}}(f) = (2\pi^2/3H_0^2)f^2h_c^2(f)$, and approximated as a power-law form:

$$h_c(f) = A_{\text{CP}} \left(\frac{f}{f_{\text{yr}}}\right)^{(3-\gamma_{\text{CP}})/2}, \quad (3.24)$$

where A_{CP} refers to the amplitude at the frequency $f = f_{\text{yr}} = 1 \text{ yr}^{-1}$. When the spectral tilt at the pulsar timing scale is the same as the one at the CMB scale, power-law index

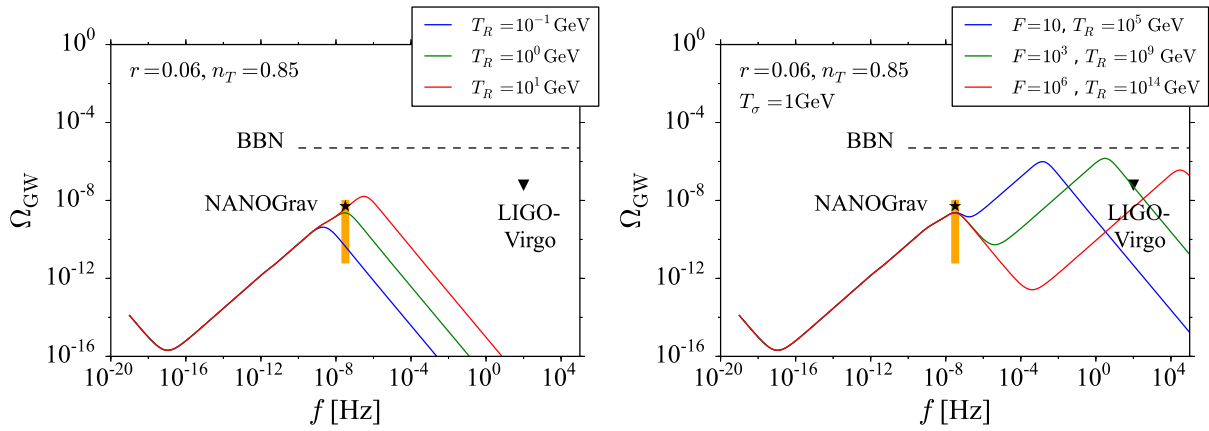


Figure 1: Examples of spectra of IGWs for the scenarios with the standard reheating (left) and late-time entropy production (right). The amplitude of the SGWB indicated by the recent NANOGrav results (orange colored region) and the current upper bounds by BBN (black dashed line) and LIGO-Virgo (black triangle) are also shown. Note that the NANOGrav results give $A_{CP} = 1.92 \times 10^{-15}$ (median value) for a $f^{-2/3}$ power-law spectrum (black star), while a larger range of A_{CP} is allowed if we consider different spectral tilt.

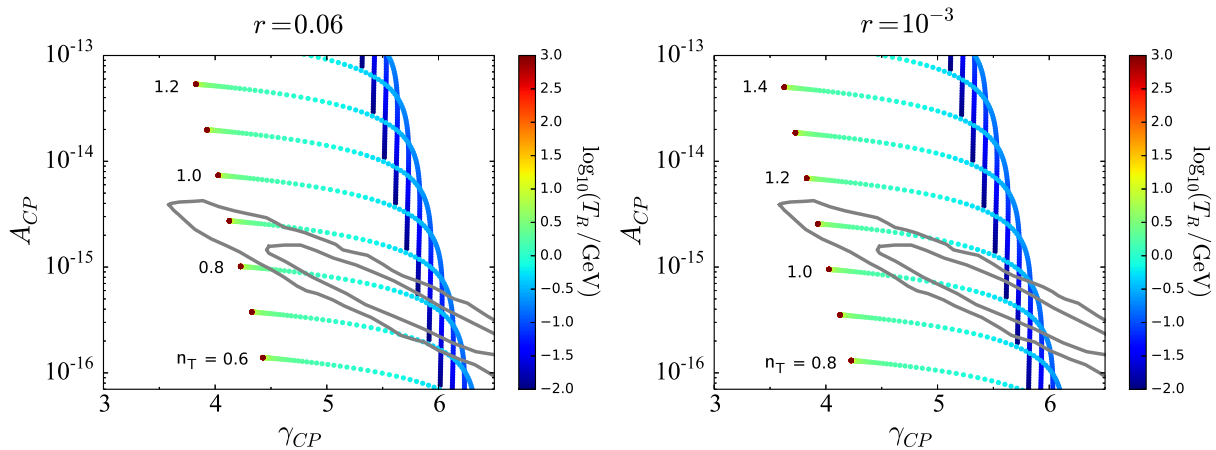


Figure 2: Predictions of the IGWs with a blue-tilted spectrum for the standard reheating scenario. We scan over the spectral tilt n_T and reheating temperature T_R projected into the $\gamma_{CP} - A_{CP}$ plane, where A_{CP} is the characteristic GW strain amplitude at $f = 1\text{yr}^{-1}$ and γ_{CP} is the spectral index of the pulsar timing-residual cross-power spectral density. We fix the value of the tensor-to-scalar ratio at $r = 0.06$ in the left panel and $r = 10^{-3}$ in the right panel. The gray curves are the 1σ and 2σ posterior contours obtained by NANOGrav based on the five-frequency power-law fit [2].

γ_{CP} can be related to n_T as $\gamma_{\text{CP}} = 5 - n_T$. On the other hand, the value of γ_{CP} deviates from $5 - n_T$ if the spectral shape is altered due to the change of Hubble expansion rate during reheating and late-time entropy production.^{#5}

In Fig. 2, we show the parameter scan in the $\gamma_{\text{CP}} - A_{\text{CP}}$ plane shown with the 1σ and 2σ posterior contours of the NANOGrav results obtained from the five-frequency power-law fit [2]. In the left and right panels, the tensor-to-scalar ratio is fixed as $r = 0.06$ and 10^{-3} , respectively. The predictions for A_{CP} and γ_{CP} are shown for several values of n_T , corresponding to the curves from the bottom (low n_T) to the top (high n_T), and different values of reheating temperature T_R , represented by different colors.

As expected, the amplitude of IGWs at the pulsar timing frequency A_{CP} gets larger for increasing n_T . We see from the colors that the dots degenerate at the same place when $T_R \gtrsim 10$ GeV, because in this case, the effect of reheating appears at frequencies higher than f_{yr} and the spectrum at the pulsar timing frequency stays the same. On the other hand, when $T_R \lesssim 10$ GeV, the value of γ_{CP} gets larger for smaller reheating temperatures since the spectrum becomes red-tilted at the pulsar timing frequency because of the bending in the spectrum induced by reheating. We see that the spectrum gets flattened (corresponding to $\gamma_{\text{CP}} = 5$) when $T_R \sim 1$ GeV, and the curve with constant n_T converges to the line of $\gamma_{\text{CP}} = 7 - n_T$ for smaller T_R , since reheating induces the extra frequency dependence of f^{-2} . Here, we take the lowest reheating temperature to be $T_R = 10^{-2}$ GeV for not interrupting the BBN epoch [60, 61].

As seen from the figure, for the case of $r = 0.06$, the NANOGrav signal can be IGWs for a broad range of reheating temperatures when the tensor spectral index is $n_T \sim 0.8$. Even when $n_T \sim 1.2$, if the reheating temperature is as low as the minimally allowed value by BBN, $T_R \sim 10^{-2}$ GeV, they can also account for the NANOGrav results. When we assume a different value for r , the values of n_T and T_R required to explain the NANOGrav signal are shifted, but the tendency is the same as seen by comparing the left and right panels of Fig. 2.

However, as already mentioned in the introduction, when we consider a blue-tilted tensor spectrum, we should also take into account the upper bound on the amplitude of the SGWB by BBN and LIGO-Virgo. In Fig. 3, we show the parameter space in the $n_T - T_R$ plane consistent with the NANOGrav results (i.e., parameter values which give prediction of γ_{CP} and A_{CP} falling inside the 2σ posterior contour shown in Fig. 2) with green color for the cases of $r = 0.06$ (left), 10^{-3} (middle), and 10^{-6} (right). Regions excluded by BBN and LIGO-Virgo are also depicted with light gray and red colors, respectively. One can see that a large region of the parameter space is indeed excluded by the BBN and LIGO-Virgo bounds, which typically is seen for high reheating temperature since the spectral amplitude continues to grow towards high frequencies. However, the figure illustrates the main message of this paper that, when one assumes relatively low reheating temperature (e.g.

^{#5}Note that the effect of g_* change is seen around the pulsar timing frequencies, not at $f \sim f_{\text{yr}}$ but around $f \sim 0.1 \text{ yr}^{-1}$ [42]. This could slightly change the value of γ_{CP} when we consider broad frequency range, but in our analysis, we estimate the spectral tilt at $f = f_{\text{yr}}$ and thus the g_* change does not affect the value of γ_{CP} .

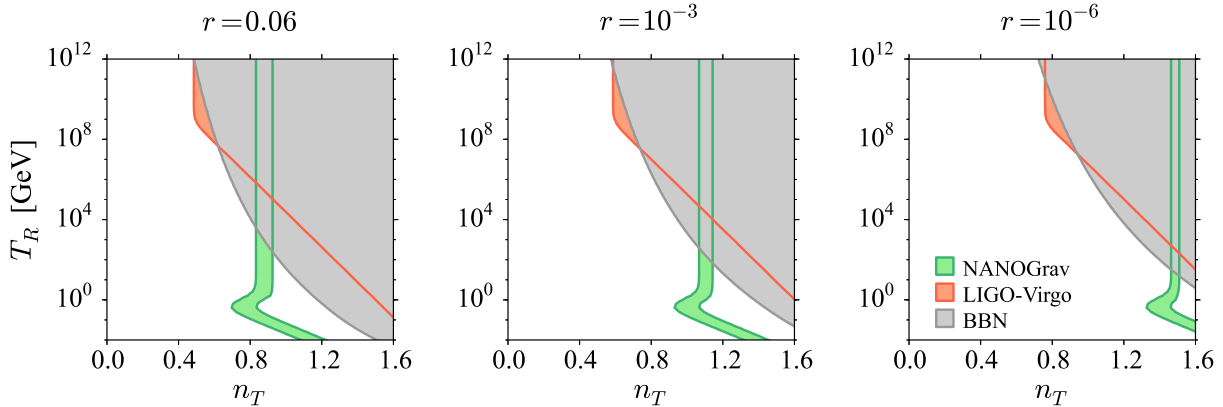


Figure 3: Parameter space consistent with the NANOGGrav results (green colored region) is shown in the n_T - T_R plane for the standard reheating scenario. The red and light gray colored regions are excluded by the current constraints from LIGO-Virgo and BBN, respectively. We show the cases for different values of the tensor-to-scalar ratio, $r = 0.06, 10^{-3}, 10^{-6}$.

($T_R < 10^3$ GeV for $r = 0.06$), the spectral amplitude gets suppressed at high frequencies and IGWs can still account for NANOGGrav signal without conflicting with the BBN and LIGO-Virgo constraints.

In the figure, we find that a higher value of n_T is required for $T_R < 1$ GeV. This is because the suppression of the GW amplitude by the MD phase occurs at the pulsar timing frequency when $T_R < 1$ GeV, and a higher value of n_T is needed to amplify GWs for explaining the NANOGGrav results. Different panels show the cases of different values of the tensor-to-scalar ratio. For a smaller value of r , we find the tendency that it requires a larger value of n_T to explain the NANOGGrav results in order to compensate for the overall suppression of the spectral amplitude. In this case, a lower reheating temperature is required to be consistent with the BBN bound, since the spectrum grows more quickly towards high frequencies when n_T is larger.

3.2 Case with late-time entropy production

Let us turn to the case with the late-time entropy production scenario. Since the Universe experiences MD phase twice before the BBN epoch in this case, the spectrum of IGWs gets more suppression as shown in the right panel of Fig. 1. Therefore the BBN and LIGO-Virgo constraints become less stringent compared to the case with the standard reheating scenario. In Fig. 4, we show the parameter space consistent with the NANOGGrav results as well as the excluded regions by BBN and LIGO-Virgo in the n_T - T_R plane. The second reheating temperature is set as $T_\sigma = 10$ GeV. Different panels show the cases of different parameter values $r = 0.06, 10^{-3}$ and $F = 10, 10^3, 10^6$.

As expected, the parameter space which can explain the NANOGrav results being consistent with the BBN and LIGO-Virgo constraints is broadened. We find that, for $r = 0.06$, the reheating temperature T_R can be as high as $T_R = 10^8$ GeV for $F = 10^3$. Interestingly, much higher reheating temperature, even $T_R \sim 10^{15}$ GeV which is close to the reheating temperature of instant reheating, is allowed if $F = 10^6$.

The dark gray region represents the requirement that the reheating temperature T_R should be higher than the temperature when the σ -oscillation dominated epoch starts, $T_{\sigma R}$. Assuming entropy conservation from T_R to $T_{\sigma R}$, we can replace $s(T_R)a^3(T_R)$ with $s(T_{\sigma R})a^3(T_{\sigma R})$ in the definition of F , Eq. (2.19). Using $s \propto T^3$ and $a^3 \propto \rho^{-1} \propto T^{-4}$ during the entropy production phase, we find that the requirement is

$$T_R > T_{\sigma R} = T_{\sigma} F. \quad (3.25)$$

4 Conclusion

In this paper, we have investigated the implications of the recent NANOGrav results for IGWs with a blue-tilted primordial spectrum by taking into account the thermal history of the Universe after inflation. We first investigated the case of the standard reheating scenario where the MD (inflaton-oscillation dominated) phase lasts for a certain period after inflation. If the MD phase lasts long enough, the GW spectrum gets suppressed at high frequencies, and hence we can avoid the BBN and LIGO-Virgo constraints. We have shown that IGWs can explain the NANOGrav results without conflicting with the BBN and LIGO-Virgo constraints when the reheating temperature is relatively low, which can be read off from Fig. 3. We found that, for $r = 0.06$, $T_R \lesssim 10^3$ GeV is required to avoid the BBN constraint. We need slightly lower reheating temperature for lower value of the tensor to scalar ratio; $T_R \lesssim 10^2$ GeV for $r = 10^{-3}$ and $T_R \lesssim 10$ GeV for $r = 10^{-6}$.

We further considered thermal history with late-time entropy production. In this scenario, MD phases appear twice between the end of inflation and BBN epoch, and hence the amplitude of IGWs at higher frequencies gets more suppressed than the standard reheating case, which makes the constraints from BBN and LIGO-Virgo less stringent. As shown in Fig. 4, the parameter space consistent with the NANOGrav results and allowed by BBN and LIGO-Virgo is enlarged compared to the standard reheating case. In particular, when $F = 10^6$ with $T_{\sigma} = 10$ GeV and $r = 0.06$, IGWs can account for the NANOGrav signal even for instant reheating, which corresponds to $T_R \sim 10^{15}$ GeV.

Although detection of quadrupole correlations is essential to claim the discovery of the SGWB by pulsar timing arrays and further observation is needed, once the NANOGrav signal is confirmed, our result would help to test inflationary cosmology via GWs and advance our understanding of the early universe. Beyond pulsar timing, measurement of a SGWB at different frequencies by CMB B-mode polarization and future interferometer experiments (e.g. LISA, DECIGO, and Einstein Telescope) would also be crucial for testing IGWs with a blue-tilted spectrum. Such multi-frequency band observations of GWs would open up a new era in GW cosmology.

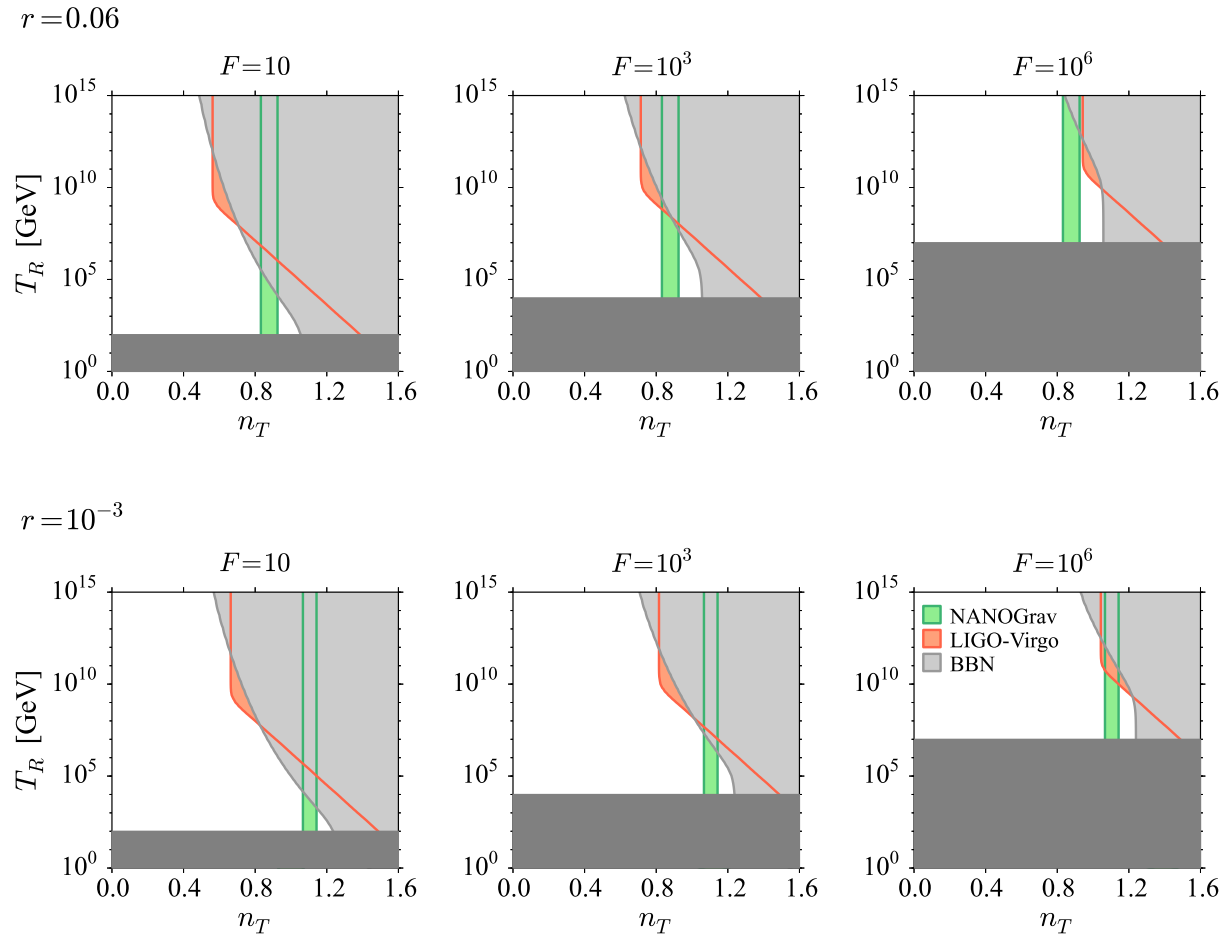


Figure 4: Parameter space consistent with the NANOGraV results (green colored region) is shown in the n_T - T_R plane for the late-time entropy production scenario. The red and light gray colored regions are excluded by the current constraints from LIGO-Virgo and BBN, respectively. The second reheating temperature is set as $T_\sigma = 10$ GeV and we show the cases for different parameter sets; $F = 10$ (left), 10^3 (middle), 10^6 (right) and $r = 0.06$ (upper), 10^{-3} (lower). The region covered by dark gray is not allowed because reheating temperature should be larger than the temperature of the Universe at the onset of σ -oscillation dominated epoch (see the text for details).

Acknowledgements

This work is supported by JSPS KAKENHI Grant Numbers 20H01899 (SK), 20J40022 (SK), 17H01131 (TT), 19K03874 (TT), 20H01932 (SY), 20K03968 (SY) and MEXT KAKENHI Grant Number 19H05110 (TT). SK is supported by the Atracción de Talento contract no. 2019-T1/TIC-13177 granted by the Comunidad de Madrid in Spain.

References

- [1] S. Kuroyanagi, T. Chiba, and T. Takahashi, *Probing the Universe through the Stochastic Gravitational Wave Background*, *JCAP* **11** (2018) 038, [[arXiv:1807.00786](#)].
- [2] NANOGrav Collaboration, Z. Arzoumanian et al., *The NANOGrav 12.5-year Data Set: Search For An Isotropic Stochastic Gravitational-Wave Background*, [arXiv:2009.04496](#).
- [3] NANOGrav Collaboration, N. S. Pol et al., *Astrophysics Milestones For Pulsar Timing Array Gravitational Wave Detection*, [arXiv:2010.11950](#).
- [4] S. Blasi, V. Brdar, and K. Schmitz, *Has NANOGrav found first evidence for cosmic strings?*, [arXiv:2009.06607](#).
- [5] J. Ellis and M. Lewicki, *Cosmic String Interpretation of NANOGrav Pulsar Timing Data*, [arXiv:2009.06555](#).
- [6] V. Vaskonen and H. Veermäe, *Did NANOGrav see a signal from primordial black hole formation?*, [arXiv:2009.07832](#).
- [7] V. De Luca, G. Franciolini, and A. Riotto, *NANOGrav Hints to Primordial Black Holes as Dark Matter*, [arXiv:2009.08268](#).
- [8] Y. Nakai, M. Suzuki, F. Takahashi, and M. Yamada, *Gravitational Waves and Dark Radiation from Dark Phase Transition: Connecting NANOGrav Pulsar Timing Data and Hubble Tension*, [arXiv:2009.09754](#).
- [9] W. Buchmuller, V. Domcke, and K. Schmitz, *From NANOGrav to LIGO with metastable cosmic strings*, [arXiv:2009.10649](#).
- [10] A. Addazi, Y.-F. Cai, Q. Gan, A. Marciano, and K. Zeng, *NANOGrav results and Dark First Order Phase Transitions*, [arXiv:2009.10327](#).
- [11] W. Ratzinger and P. Schwaller, *Whispers from the dark side: Confronting light new physics with NANOGrav data*, [arXiv:2009.11875](#).
- [12] K. Kohri and T. Terada, *Solar-Mass Primordial Black Holes Explain NANOGrav Hint of Gravitational Waves*, [arXiv:2009.11853](#).
- [13] R. Samanta and S. Datta, *Gravitational wave complementarity and impact of NANOGrav data on gravitational leptogenesis: cosmic strings*, [arXiv:2009.13452](#).
- [14] S. Vagnozzi, *Implications of the NANOGrav pulsar timing results for inflation*, [arXiv:2009.13432](#).

- [15] A. Neronov, A. Roper Pol, C. Caprini, and D. Semikoz, *NANOGrav signal from MHD turbulence at QCD phase transition in the early universe*, [arXiv:2009.14174](#).
- [16] L. Bian, J. Liu, and R. Zhou, *NanoGrav 12.5-yr data and different stochastic Gravitational wave background sources*, [arXiv:2009.13893](#).
- [17] R. Namba and M. Suzuki, *Implications of Gravitational-wave Production from Dark Photon Resonance to Pulsar-timing Observations and Effective Number of Relativistic Species*, [arXiv:2009.13909](#).
- [18] H.-H. Li, G. Ye, and Y.-S. Piao, *Is the NANOGrav signal a hint of dS decay during inflation?*, [arXiv:2009.14663](#).
- [19] S. Sugiyama, V. Takhistov, E. Vitagliano, A. Kusenko, M. Sasaki, and M. Takada, *Testing Stochastic Gravitational Wave Signals from Primordial Black Holes with Optical Telescopes*, [arXiv:2010.02189](#).
- [20] G. Domènech and S. Pi, *NANOGrav Hints on Planet-Mass Primordial Black Holes*, [arXiv:2010.03976](#).
- [21] S. Bhattacharya, S. Mohanty, and P. Parashari, *Implications of the NANOGrav result on primordial gravitational waves in nonstandard cosmologies*, [arXiv:2010.05071](#).
- [22] K. T. Abe, Y. Tada, and I. Ueda, *Induced gravitational waves as a cosmological probe of the sound speed during the QCD phase transition*, [arXiv:2010.06193](#).
- [23] N. Kitajima, J. Soda, and Y. Urakawa, *Nano-Hz gravitational wave signature from axion dark matter*, [arXiv:2010.10990](#).
- [24] K. Inomata, M. Kawasaki, K. Mukaida, and T. T. Yanagida, *NANOGrav results and LIGO-Virgo primordial black holes in axion-like curvaton model*, [arXiv:2011.01270](#).
- [25] H. W. Tahara and T. Kobayashi, *Nanohertz gravitational waves from NEC violation in the early universe*, [arXiv:2011.01605](#).
- [26] A. Gruzinov, *Elastic inflation*, *Phys. Rev. D* **70** (2004) 063518, [[astro-ph/0404548](#)].
- [27] M. Satoh and J. Soda, *Higher Curvature Corrections to Primordial Fluctuations in Slow-roll Inflation*, *JCAP* **09** (2008) 019, [[arXiv:0806.4594](#)].
- [28] T. Kobayashi, M. Yamaguchi, and J. Yokoyama, *G-inflation: Inflation driven by the Galileon field*, *Phys. Rev. Lett.* **105** (2010) 231302, [[arXiv:1008.0603](#)].
- [29] S. Endlich, A. Nicolis, and J. Wang, *Solid Inflation*, *JCAP* **10** (2013) 011, [[arXiv:1210.0569](#)].

- [30] S. Koh, B.-H. Lee, W. Lee, and G. Tumurtushaa, *Observational constraints on slow-roll inflation coupled to a Gauss-Bonnet term*, *Phys. Rev. D* **90** (2014), no. 6 063527, [[arXiv:1404.6096](#)].
- [31] D. Cannone, G. Tasinato, and D. Wands, *Generalised tensor fluctuations and inflation*, *JCAP* **01** (2015) 029, [[arXiv:1409.6568](#)].
- [32] Y.-F. Cai, J.-O. Gong, S. Pi, E. N. Saridakis, and S.-Y. Wu, *On the possibility of blue tensor spectrum within single field inflation*, *Nucl. Phys. B* **900** (2015) 517–532, [[arXiv:1412.7241](#)].
- [33] A. Ricciardone and G. Tasinato, *Primordial gravitational waves in supersolid inflation*, *Phys. Rev. D* **96** (2017), no. 2 023508, [[arXiv:1611.04516](#)].
- [34] S. Koh, B.-H. Lee, and G. Tumurtushaa, *Constraints on the reheating parameters after Gauss-Bonnet inflation from primordial gravitational waves*, *Phys. Rev. D* **98** (2018), no. 10 103511, [[arXiv:1807.04424](#)].
- [35] T. Fujita, S. Kuroyanagi, S. Mizuno, and S. Mukohyama, *Blue-tilted Primordial Gravitational Waves from Massive Gravity*, *Phys. Lett. B* **789** (2019) 215–219, [[arXiv:1808.02381](#)].
- [36] Y. Mishima and T. Kobayashi, *Revisiting slow-roll dynamics and the tensor tilt in general single-field inflation*, *Phys. Rev. D* **101** (2020), no. 4 043536, [[arXiv:1911.02143](#)].
- [37] T. Nakama and T. Suyama, *Primordial black holes as a novel probe of primordial gravitational waves*, *Phys. Rev. D* **92** (2015), no. 12 121304, [[arXiv:1506.05228](#)].
- [38] T. Nakama and T. Suyama, *Primordial black holes as a novel probe of primordial gravitational waves. II: Detailed analysis*, *Phys. Rev. D* **94** (2016), no. 4 043507, [[arXiv:1605.04482](#)].
- [39] N. Seto and J. Yokoyama, *Probing the equation of state of the early universe with a space laser interferometer*, *J. Phys. Soc. Jap.* **72** (2003) 3082–3086, [[gr-qc/0305096](#)].
- [40] L. A. Boyle and P. J. Steinhardt, *Probing the early universe with inflationary gravitational waves*, *Phys. Rev. D* **77** (2008) 063504, [[astro-ph/0512014](#)].
- [41] K. Nakayama, S. Saito, Y. Suwa, and J. Yokoyama, *Probing reheating temperature of the universe with gravitational wave background*, *JCAP* **06** (2008) 020, [[arXiv:0804.1827](#)].
- [42] S. Kuroyanagi, T. Chiba, and N. Sugiyama, *Precision calculations of the gravitational wave background spectrum from inflation*, *Phys. Rev. D* **79** (2009) 103501, [[arXiv:0804.3249](#)].

- [43] S. Kuroyanagi, T. Chiba, and N. Sugiyama, *Prospects for Direct Detection of Inflationary Gravitational Waves by Next Generation Interferometric Detectors*, *Phys. Rev. D* **83** (2011) 043514, [[arXiv:1010.5246](#)].
- [44] S. Kuroyanagi, K. Nakayama, and S. Saito, *Prospects for determination of thermal history after inflation with future gravitational wave detectors*, *Phys. Rev. D* **84** (2011) 123513, [[arXiv:1110.4169](#)].
- [45] S. Kuroyanagi, K. Nakayama, and J. Yokoyama, *Prospects of determination of reheating temperature after inflation by DECIGO*, *PTEP* **2015** (2015), no. 1 013E02, [[arXiv:1410.6618](#)].
- [46] S. Kuroyanagi, T. Takahashi, and S. Yokoyama, *Blue-tilted Tensor Spectrum and Thermal History of the Universe*, *JCAP* **02** (2015) 003, [[arXiv:1407.4785](#)].
- [47] K. Nakayama and J. Yokoyama, *Gravitational Wave Background and Non-Gaussianity as a Probe of the Curvaton Scenario*, *JCAP* **01** (2010) 010, [[arXiv:0910.0715](#)].
- [48] S. Kuroyanagi, C. Ringeval, and T. Takahashi, *Early universe tomography with CMB and gravitational waves*, *Phys. Rev. D* **87** (2013), no. 8 083502, [[arXiv:1301.1778](#)].
- [49] F. D’Eramo and K. Schmitz, *Imprint of a scalar era on the primordial spectrum of gravitational waves*, *Phys. Rev. Research.* **1** (2019) 013010, [[arXiv:1904.07870](#)].
- [50] S. Kuroyanagi and T. Takahashi, *Higher Order Corrections to the Primordial Gravitational Wave Spectrum and its Impact on Parameter Estimates for Inflation*, *JCAP* **10** (2011) 006, [[arXiv:1106.3437](#)].
- [51] M. S. Turner, M. J. White, and J. E. Lidsey, *Tensor perturbations in inflationary models as a probe of cosmology*, *Phys. Rev. D* **48** (1993) 4613–4622, [[astro-ph/9306029](#)].
- [52] Y. Watanabe and E. Komatsu, *Improved Calculation of the Primordial Gravitational Wave Spectrum in the Standard Model*, *Phys. Rev. D* **73** (2006) 123515, [[astro-ph/0604176](#)].
- [53] K. Saikawa and S. Shirai, *Primordial gravitational waves, precisely: The role of thermodynamics in the Standard Model*, *JCAP* **05** (2018) 035, [[arXiv:1803.01038](#)].
- [54] **Planck** Collaboration, N. Aghanim et al., *Planck 2018 results. VI. Cosmological parameters*, *Astron. Astrophys.* **641** (2020) A6, [[arXiv:1807.06209](#)].
- [55] **Planck** Collaboration, Y. Akrami et al., *Planck 2018 results. X. Constraints on inflation*, *Astron. Astrophys.* **641** (2020) A10, [[arXiv:1807.06211](#)].

- [56] **BICEP2, Keck Array** Collaboration, P. Ade et al., *BICEP2 / Keck Array x: Constraints on Primordial Gravitational Waves using Planck, WMAP, and New BICEP2/Keck Observations through the 2015 Season*, *Phys. Rev. Lett.* **121** (2018) 221301, [[arXiv:1810.05216](#)].
- [57] M. Tristram et al., *Planck constraints on the tensor-to-scalar ratio*, [arXiv:2010.01139](#).
- [58] R. H. Cyburt, B. D. Fields, K. A. Olive, and T.-H. Yeh, *Big Bang Nucleosynthesis: 2015*, *Rev. Mod. Phys.* **88** (2016) 015004, [[arXiv:1505.01076](#)].
- [59] **LIGO Scientific, Virgo** Collaboration, B. Abbott et al., *Search for the isotropic stochastic background using data from Advanced LIGO's second observing run*, *Phys. Rev. D* **100** (2019), no. 6 061101, [[arXiv:1903.02886](#)].
- [60] M. Kawasaki, K. Kohri, and N. Sugiyama, *MeV scale reheating temperature and thermalization of neutrino background*, *Phys. Rev. D* **62** (2000) 023506, [[astro-ph/0002127](#)].
- [61] S. Hannestad, *What is the lowest possible reheating temperature?*, *Phys. Rev. D* **70** (2004) 043506, [[astro-ph/0403291](#)].